BRAIN
ORIGINAL ARTICLE

The gain of function *SCN1A* disorder spectrum: novel epilepsy phenotypes and therapeutic implications

Andreas Brunklaus,[1,2,†] Tobias Brünger,[3] Tony Feng,[1,2] Carmen Fons,[4] Anni Lehikoinen,[5] Eleni Panagiotakaki,[6] Mihaela-Adela Vintan,[7] Joseph Symonds,[1,2] James Andrew,[2] Alexis Arzimanoglou,[4,6] Sarah Delima,[8] Julie Gallois,[9] Donncha Hanrahan,[10] Gaetan Lesca,[11] Stewart MacLeod,[2] Dragan Marjanovic,[12] Amy McTague,[13,14] Noemi Nuñez-Enamorado,[15] Eduardo Perez-Palma,[16] M. Scott Perry,[17] Karen Pysden,[18] Sophie J. Russ-Hall,[19] Ingrid E. Scheffer,[19,20,21] Krystal Sully,[22,23] Steffen Syrbe,[24] Ulvi Vaher,[25] Murugan Velayutham,[26] Julie Vogt,[27] Shelly Weiss,[28] Elaine Wirrell,[29] Sameer M Zuberi,[1,2] Dennis Lal,[3,30,31,32] Rikke S. Møller,[12,33] Massimo Mantegazza[34,35,36] and Sandrine Cestèle[34,35,†]

[†]These authors contributed equally to this work.

Brain voltage-gated sodium channel $Na_V1.1$ (*SCN1A*) loss-of-function variants cause the severe epilepsy Dravet syndrome, as well as milder phenotypes associated with genetic epilepsy with febrile seizures plus. Gain of function *SCN1A* variants are associated with familial hemiplegic migraine type 3. Novel *SCN1A*-related phenotypes have been described including early infantile developmental and epileptic encephalopathy with movement disorder, and more recently neonatal presentations with arthrogryposis. Here we describe the clinical, genetic and functional evaluation of affected individuals.

Thirty-five patients were ascertained via an international collaborative network using a structured clinical questionnaire and from the literature. We performed whole-cell voltage-clamp electrophysiological recordings comparing sodium channels containing wild-type versus variant $Na_V1.1$ subunits. Findings were related to Dravet syndrome and familial hemiplegic migraine type 3 variants.

We identified three distinct clinical presentations differing by age at onset and presence of arthrogryposis and/or movement disorder. The most severely affected infants ($n = 13$) presented with congenital arthrogryposis, neonatal onset epilepsy in the first 3 days of life, tonic seizures and apnoeas, accompanied by a significant movement disorder and profound intellectual disability. Twenty-one patients presented later, between 2 weeks and 3 months of age, with a severe early infantile developmental and epileptic encephalopathy and a movement disorder. One patient presented after 3 months with developmental and epileptic encephalopathy only. Associated *SCN1A* variants cluster in regions of channel inactivation associated with gain of function, different to Dravet syndrome variants (odds ratio = 17.8; confidence interval = 5.4–69.3; $P = 1.3 \times 10^{-7}$). Functional studies of both epilepsy and familial hemiplegic migraine type 3 variants reveal alterations of gating properties in keeping with neuronal hyperexcitability. While epilepsy variants result in a moderate increase in action current amplitude consistent with mild gain of function, familial hemiplegic migraine type 3 variants induce a larger effect on gating properties, in particular the increase of persistent current, resulting in a large increase of action current amplitude, consistent with stronger gain of function.

Received January 13, 2022. Revised April 14, 2022. Accepted May 26, 2022. Advance access publication June 13, 2022

Clinically, 13 out of 16 (81%) gain of function variants were associated with a reduction in seizures in response to sodium channel blocker treatment (carbamazepine, oxcarbazepine, phenytoin, lamotrigine or lacosamide) without evidence of symptom exacerbation.

Our study expands the spectrum of gain of function *SCN1A*-related epilepsy phenotypes, defines key clinical features, provides novel insights into the underlying disease mechanisms between *SCN1A*-related epilepsy and familial hemiplegic migraine type 3, and identifies sodium channel blockers as potentially efficacious therapies. Gain of function disease should be considered in early onset epilepsies with a pathogenic *SCN1A* variant and non-Dravet syndrome phenotype.

1 Institute of Health and Wellbeing, University of Glasgow, Glasgow, UK
2 The Paediatric Neurosciences Research Group, Royal Hospital for Children, Member of the ERN EpiCARE, Glasgow, UK
3 Cologne Center for Genomics, University of Cologne, Cologne, Germany
4 Pediatric Neurology Department, CIBERER-ISCIII, Sant Joan de Déu Universitary Hospital, Institut de Recerca Sant Joan de Déu, Member of the ERN EpiCARE, Barcelona, Spain
5 Pediatric Neurology Department, Kuopio University Hospital, Member of the ERN EpiCARE, Kuopio, Finland
6 Department of Paediatric Clinical Epileptology, sleep disorders and functional neurology, Member of the ERN EpiCARE, University Hospitals of Lyon (HCL) and Inserm U1028/CNRS UMR5292, Lyon, France
7 'Iuliu Hatieganu' University of Medicine and Pharmacy, Faculty of Medicine, Department of Neuroscience, Neurology and Pediatric Neurology, Victor Babes, 43, 400012 Cluj-Napoca, Romania
8 Indiana University School of Medicine, IU Health Riley Hospital for Children, Department of Neurology, Division of Pediatric Neurology, Indianapolis, IN, USA
9 Louisiana State University Health Sciences Center School of Medicine, New Orleans, LA, USA
10 Department of Paediatric Neurology, Royal Belfast Hospital for Sick Children, Belfast, UK
11 Department of Medical Genetics, Lyon University Hospital, Member of the ERN EpiCARE, Université Claude Bernard Lyon 1, Lyon, France
12 The Danish Epilepsy Centre, Member of the ERN EpiCARE, Dianalund, Denmark
13 Developmental Neurosciences, UCL Great Ormond Street Institute of Child Health, London, UK
14 Department of Neurology, Great Ormond Street Hospital for Children, Member of the ERN EpiCARE, London, UK
15 Pediatric Neurology Department, 12 Octubre Universitary Hospital, Madrid, Spain
16 Universidad del Desarrollo, Centro de Genética y Genómica, Facultad de Medicina Clínica Alemana, Santiago, Chile
17 Jane and John Justin Neurosciences Center, Cook Children's Medical Center, Ft Worth, TX, USA
18 Paediatric Neurology Department, Leeds Teaching Hospitals, Leeds General Infirmary, Leeds, UK
19 Epilepsy Research Centre, Department of Medicine, University of Melbourne, Austin Health, Melbourne, Australia
20 Florey Institute of Neuroscience and Mental Health, Melbourne, Australia
21 Murdoch Children's Research Institute and Department of Paediatrics, University of Melbourne, Royal Children's Hospital, Melbourne, Australia
22 Baylor College of Medicine, Houston, TX, USA
23 Texas Children's Hospital, Houston, TX, USA
24 Division of Pediatric Epileptology, Center for Pediatrics and Adolescent Medicine, University Hospital Heidelberg, Heidelberg, Germany
25 Children's Clinic of Tartu University Hospital, Faculty of Medicine of Tartu University, Member of the ERN EpiCARE, Tartu, Estonia
26 Birmingham Children's Hospital, Birmingham, UK
27 West Midlands Regional Genetics Service, Birmingham Women's and Children's Hospital, Birmingham, UK
28 Division of Neurology, SickKids, University of Toronto, Toronto, Canada
29 Divisions of Epilepsy and Child and Adolescent Neurology, Department of Neurology, Mayo Clinic, Rochester, MN, USA
30 Genomic Medicine Institute, Lerner Research Institute, Cleveland Clinic, Cleveland, OH, USA
31 Epilepsy Center, Neurological Institute, Cleveland Clinic, Cleveland, OH, USA
32 Stanley Center for Psychiatric Genetics, Broad Institute of MIT and Harvard, Cambridge, MA, USA
33 Department of Regional Health Research, University of Southern Denmark, Odense, Denmark
34 Université Côte d'Azur, 06560 Valbonne-Sophia Antipolis, France
35 CNRS UMR7275, Institute of Molecular and Cellular Pharmacology (IPMC), 06560 Valbonne-Sophia Antipolis, France
36 Inserm, 06560 Valbonne-Sophia Antipolis, France

Correspondence to: Professor Andreas Brunklaus, MD
Institute of Health and Wellbeing University of Glasgow
Paediatric Neurosciences Research Group
Office Block, Ground Floor, Zone 2
Royal Hospital for Children 1345 Govan Road, Glasgow G51 4TF, UK
E-mail: andreas.brunklaus@glasgow.ac.uk

Correspondence may also be addressed to: Professor Rikke Steensbjerre Møller, PhD
E-mail: rimo@filadelfia.dk

Professor Massimo Mantegazza, PhD
E-mail: mantegazza@ipmc.cnrs.fr

Professor Sandrine Cestèle, PhD
E-mail: cestele@ipmc.cnrs.fr

Keywords: *SCN1A*; gain of function; epilepsy; arthrogryposis; movement disorder

Introduction

Voltage-gated sodium (Na^+) channels are transmembrane proteins that play a major role in the initiation and propagation of action potentials in neurons and electrically excitable tissues.[1] There are four primarily brain-expressed Na^+ channel genes including *SCN1A*, *SCN2A*, *SCN3A* and *SCN8A* that have been associated with epilepsy and neurodevelopmental disorders.[2–6] Disease presentations relate to the underlying change in functional properties [gain- versus loss-of-function (GOF versus LOF)] of affected neurons, which can guide treatment.[1,7]

LOF variants in the *SCN1A* gene cause Dravet syndrome, one of the most common monogenic epilepsies, and genetic epilepsy with febrile seizures plus (GEFS+).[2,8–10] While children with Dravet syndrome present with severe drug-resistant epilepsy and significant intellectual disability,[11,12] individuals with GEFS+ phenotypes have well controlled epilepsy with normal cognition.[13] These disorders lie at different ends of the *SCN1A*-disease spectrum reflecting the degree of LOF in inhibitory interneurons. Given the underlying LOF disease mechanism, individuals typically experience seizure exacerbation following sodium channel blocker (SCB) use.[9,10,14–17]

By contrast, GOF *SCN1A* variants are associated with familial hemiplegic migraine type 3 (FHM3).[18–20] Individuals present with a severe subtype of migraine with aura characterized by hemiparesis during the attacks.[18,19]

A more severe *SCN1A* phenotype of early infantile developmental and epileptic encephalopathy (EIDEE) with onset of seizures ≤3 months, profound developmental impairment and a hyperkinetic movement disorder (MD) has been described.[21] Most cases had the recurrent *SCN1A* missense variant p.T226M. This variant had different biophysical properties to those observed in Dravet syndrome or GEFS+. T226M demonstrated mixed GOF and LOF properties, including a GOF hyperpolarizing shift in activation accompanied by a LOF hyperpolarizing shift in inactivation and depolarizing block.[22] None of the affected patients responded to SCB treatment.

Recently, a series of three patients with antenatal diagnosis of arthrogryposis multiplex congenita (AMC) was identified, all carrying *de novo* *SCN1A* variants. Individuals either died *in utero* or presented with drug-resistant epileptic seizures from birth.[23]

It is currently unknown how *SCN1A* variants contribute to this profound disease phenotype. Clarification of the underlying disease mechanism is paramount as this will inform treatment choice. Importantly, new *SCN1A* directed disease modifying therapies are being developed that target LOF variants.[24] Such treatments would be contraindicated in patients with GOF disease.

Here, we provide new clinical, genetic and biophysical evidence that GOF *SCN1A* diseases expand beyond FHM3 phenotypes, encompassing a wider spectrum, ranging from neonatal DEE with MD and arthrogryposis to patients with early infantile DEE with or without MD. The majority of these patients respond to sodium channel blocking therapies.

Materials and methods

Study design

This study was designed to determine the clinical characteristics and the underlying biophysical mechanisms associated with phenotypes of patients with neonatal and EIDEE with arthrogryposis and/or MD, to understand how these differ from patients presenting with Dravet syndrome and familial hemiplegic migraine (FHM3) and to evaluate treatment response in patients with *SCN1A* GOF variants. To achieve these aims, we undertook clinical and genetic evaluations of affected individuals, performed a systematic literature search to identify additional cases, functionally characterized *SCN1A* variants via patch-clamp recordings and identified likely efficacious treatments for patients with *SCN1A* GOF variants. Sample sizes for electrophysiological studies were determined on the basis of previous work and are detailed with *P* values in figure legends. Additional detailed clinical descriptions of study participants are reported in the Supplementary material. Retrospective review of anonymized clinical data and variant findings was approved by the West of Scotland Research Ethics Committee (reference number: 16/WS/0203). Informed consent for participation was provided by participants, parents or legal guardians of adults unable to consent for themselves and the appropriate institutional forms have been archived. The authors affirm that human research participants or their parents or guardians provided informed consent for publication of the images in Fig. 2 and Supplementary Videos 1–4. Consent and collection of information conformed to the recognized standards of the Declaration of Helsinki.

Clinical and genetic evaluations of previously unpublished patients

Twenty previously unreported patients with a pathogenic *SCN1A* variants and phenotypes in keeping with either very early onset ≤3 months, arthrogryposis and/or a MD were included in this study. Patients were ascertained via an international network of collaborating clinicians and geneticists. Referring clinicians completed a structured clinical questionnaire for every patient detailing medical and developmental history, neurological examination, EEG and neuroimaging findings. Seizure types were diagnosed according to the International League against epilepsy classification criteria, and were assigned, where possible, to defined epileptic syndromes.[25,26] The response to treatment was retrospectively classified according to the judgement of the treating clinician into seizure freedom, seizure reduction, no effect or seizure worsening. Particular attention was given to the effects of SCBs defined as antiseizure medications that reduce the activity of sodium channels including phenytoin, carbamazepine, oxcarbazepine, lamotrigine and lacosamide. Missense variants in *SCN1A* were identified in research or diagnostic laboratories via next-generation sequencing panel

testing and validated by Sanger sequencing. Variants were classified according to the 2015 American College of Medical Genetics and Genomics/Association for Molecular Pathology Guidelines[27] (Supplementary Table 1). Variants were assumed to be pathogenic if they were predicted to be damaging by one or more prediction software packages (PolyPhen-2, SIFT, MutationTaster, CADD[28] and REVEL[29]) and not observed in gnomAD (the genome aggregation database) (Supplementary Table 1).

Systematic literature search

In accordance with PRISMA guidance, we searched PubMed up until 31 October 2021 using the term '*SCN1A*' for any patients presenting with phenotypes consistent with very 'early onset seizures' (defined as onset ≤3 months), 'arthrogryposis', a 'MD' or 'FHM' (or 'FHM3' or 'familial hemiplegic migraine'), and included all relevant patient-related information in our dataset. For patients with little or no clinical information, we listed the phenotype mentioned in the respective publication. We included GOF FHM3 cases whose variants were electrophysiologically characterized by whole-cell patch-clamp experiments in mammalian cell lines. To compare the distribution of early onset DEE variants with those of Dravet syndrome across $Na_V1.1$ we used *SCN1A* missense variants from a published cohort of patients with Dravet syndrome.[30]

Functional characterization of *SCN1A* variants

Site-directed mutagenesis: The human clone of the shorter splice variant isoform (1998 aa) of the $Na_V1.1$ sodium channel subcloned into the plasmid pCDM8[31] was used to perform mutagenesis as previously described.[32–34] Briefly, variants were introduced into pCDM8-$hNa_V1.1$ by means of the Quick Change XL site-directed mutagenesis kit (Stratagene). Colonies were screened by sequencing and the whole open reading frame of $hNa_V1.1$ was sequenced after each propagation to exclude the presence of spurious variants.

Cell culture and transfection

The cell line tsA-201 (human embryonic kidney-293T) was maintained and transiently transfected with $CaPO_4$ as already reported.[32] Cells were cotransfected with the cDNA of $hNa_V1.1$ and a reporter vector expressing Yellow Fluorescent Protein (pEYFP-N1; Clontech) to identify the transfected cells for electrophysiological recordings.

Electrophysiological recordings and analysis

Sodium currents were recorded using the whole-cell configuration of the patch-clamp technique. Cells were recorded at room temperature (20–24°C) using a MultiClamp 700A amplifier and pClamp 10.2 software (Axon Instruments/Molecular Devices). Signals were filtered at 10 kHz and sampled at 50 kHz. Electrode capacitance and series resistance were carefully compensated during the experiment. Pipette resistance was ∼2–2.5 MΩ and maximal accepted voltage-clamp error was <2.5 mV. The remaining transient and leakage currents were eliminated using a P/4 subtraction paradigm. Recording solutions were (in mM): external solution 150 NaCl, 1 $MgCl_2$, 1.5 $CaCl_2$ and 10 HEPES (pH 7.4 with NaOH); internal pipette solution 105 CsF, 35 NaCl, 10 EGTA, 10 HEPES and (pH 7.4 with CsOH). Voltage dependence of activation was studied applying test pulses of 100-ms from −110 to +60 mV from a holding potential at −120 mV. Voltage dependence of inactivation was studied with a 100-ms prepulse at different potentials followed by a test pulse at −10 mV. Conductance–voltage curves were derived from current–voltage (*IV*) curves according to $G = I/(V - V_r)$, where I is the peak current, V is the test voltage and V_r is the apparent observed reversal potential. The voltage dependence of activation and the voltage dependence of inactivation were fit to Boltzmann relationships in the form $y = 1/(1 + \exp((V_{½} - V)/k))$, where y is normalized G_{Na} or I_{Na}, $V_{½}$ is the voltage of half-maximal activation (V_a) or inactivation (V_h) and k is a slope factor; for the inactivation curve, we included a baseline. The kinetics of current decay was quantified at −10 mV fitting the first 10 ms of the decay with a single exponential function. Recovery from fast inactivation was studied using a test pulse at 0 mV followed by a repolarization at −80 mV of increasing duration and a test pulse to 0 mV; the τ was obtained fitting the recovery curve with a single exponential function. The persistent current (I_{NaP}) was quantified about 5 min after obtaining the whole-cell configuration as the mean current between 73.5 and 78.5 ms after the beginning of a voltage step to −10 mV. Ramp currents were elicited with a 50 mV/s depolarizing ramp from −60 to +10 mV. Kinetics of development of fast inactivation was quantified with a step to −60 mV (duration between 0 and 80 ms, 5 ms increments) followed by a test pulse to 0 mV. Action potential-clamp recordings were performed as already described.[32] The intersweep interval was 8 s for all the protocols. Data were analysed with pClamp v.10.2 (Axon Instruments/Molecular Devices) and Origin2021 (OriginLab). Junction potential was not corrected.

In silico functional variant interpretation

In cases where biophysical experimental data were not available, several tools have been used to estimate function. It has recently been shown that variant function and location within one sodium channel can serve as a surrogate for variant effects across related sodium channels.[7,35] If an identical missense variant in a paralogue sodium channel has been functionally characterized, findings are likely to apply to the new variant. In addition, we used a recently developed *in silico* functional prediction tool functional variant prediction in Navs and Cavs ion channels or funNCion (https://funnc.shinyapps.io/shinyappweb/) to estimate biophysical properties[36] and used the PER viewer (http://per.broadinstitute.org/) to assess whether a specific variant location has been associated with primary GOF or LOF disease.[37]

Statistical analysis

Electrophysiological measurements were taken from distinct samples. Normality was tested with the Kolmogorov–Smirnov test; and homogeneity of variance with the Levene's test. Groups were compared with one-way ANOVA and Tukey's *post hoc* test. Data in Fig. 5F were not homoscedastic, thus we have analysed them with the Kruskal–Wallis test followed by the Dunn's *post hoc* test. We conducted a two-sided Fisher's exact test to quantify the burden of variants associated with early onset DEE versus Dravet syndrome in different regions of the SCN1A protein. Differential spatial distribution of variants on SCN1A protein structure was calculated using a paired Wilcoxon rank-sum test comparing the average distance of variant-associated residues within each phenotype group to the average distance of the combined set. We applied the Bonferroni correction to adjust for multiple testing. Significance was tested at the 5% level and analysis was performed using R version 4.1.0.

Data availability

All data associated with this study are present in the paper or the Supplementary material. Raw data for electrophysiological experiments will be deposited in a public repository (Zenodo).

Results

Early onset DEE variants cluster in channel regions associated with GOF

A cohort of 35 individuals with early onset DEE who harbour 22 heterozygous variants in *SCN1A* was identified via next-generation sequencing panel testing ($n = 20$) and systematic literature search ($n = 15$, Supplementary Tables 1–3).[21–23,38–41] All variants affected amino acid residues that are highly conserved across paralogous human Na^+ channel genes, were absent from gnomAD and predicted to be damaging by *in silico* prediction tools (Supplementary Table 1). Variants cluster in regions of channel inactivation (S4-5 and D3-4 linker) that are often associated with GOF (Fig. 1A).[36] In comparison, *SCN1A* missense variants from a published cohort of Dravet syndrome patients ($n = 440$)[30] have a different distribution and are frequently located in pore regions (S5-6) associated with LOF [Fig. 1B; odds ratio (OR) = 17.8; confidence interval (CI) = 5.4–69.3; $P = 1.3 \times 10^{-7}$].[36]

SCN1A GOF variant carriers present with a spectrum of early onset developmental and epileptic encephalopathies

We identified three distinct clinical presentations among this patient cohort differing by age at onset and presence of AMC and/or MD (Supplementary Tables 1–3).

Neonatal developmental and epileptic encephalopathy with MD and arthrogryposis (NDEEMA)

We delineated the clinical spectrum of this novel phenotype among eight previously unpublished patients. Through our literature search, we recognized this phenotype in five additional cases, comprising three antenatal AMC cases, a single report of early infantile epileptic encephalopathy and a case description of epilepsy of infancy with migrating focal seizures (Supplementary Table 2). AMC was identified *in utero* or after birth with either upper, lower or multiple limb contractures (Fig. 2). Two patients died *in utero* (Patients 5 and 9). Patients experienced neonatal onset epilepsy in the first 3 days of life including tonic seizures and apnoeas (Supplementary Fig. 1; Patient 4). Additional seizure types included focal clonic, epileptic spasms, eyelid myoclonia (Supplementary Video 1; Patient 12), generalized tonic-clonic seizures and status epilepticus. Many patients experienced reflex seizures triggered by environmental stimuli (touch, noise). Multi-focal discharges were seen on EEG as well as migrating patterns and generalized spike-wave. Non-convulsive status epilepticus and continuous spike-wave during sleep often emerged after the first year of life (Supplementary Fig. 2; Patients 1 and 4). All patients developed a MD within the first 2 years of life including hyperkinetic and choreiform movements (Supplementary Video 2; Patient 12) as well as non-epileptic myoclonus. Early MRI was normal with subsequent imaging showing progressive cortical atrophy in one individual. Four children had osteopenia with bone fractures and three compensated metabolic acidosis. Patients are currently between 2 and 6 years of age, all have profound intellectual disability, either since birth or due to later regression, and are non-ambulant and non-verbal. The epilepsy has been drug-resistant in all. However, eight out of nine (89%) variant carriers experienced a reduction in seizures (p.T162I, p.S228P, p.V229L, p.I236V, p.L247V, p.I883T, p.A1339D, p.S1346P) in response to SCB treatment (carbamazepine, phenytoin, lacosamide, oxcarbazepine). There was no reported worsening of seizures in response to SCB use (Supplementary Table 2 and Supplementary material). We call this newly recognized disease entity NDEEMA.

EIDEE and MD

We identified 10 unpublished patients and 11 individuals from the literature with a phenotype of EIDEE and MD without AMC (Supplementary Table 3). Fifteen patients harboured the two recurrent variants p.T226M ($n = 10$) and p.R1636Q ($n = 5$). Children presented between 2 weeks and 3 months of age with tonic seizures, apnoeas and focal clonic seizures, often triggered by environmental stimuli, but rarely fever. Subsequent seizure types included generalized tonic-clonic, myoclonic seizures and status epilepticus. The EEG showed multi-focal discharges and generalized spike-wave. Prominent eyelid myoclonia were noted in early childhood, as well as non-convulsive status epilepticus (Supplementary Videos 3 and 4; Patient 24). A MD including hyperkinesia, chorea, dystonia and myoclonus emerged in all patients within the first 2 years of life. MRIs of the brain were unremarkable, however some individuals developed progressive atrophy and acquired microcephaly. One child had osteopenia with bone fractures. At last follow-up, individuals were between 1 and 23 years of age. Six patients (29%) had died (Supplementary Table 3). All patients had severe to profound intellectual disability, most were non-verbal and non-ambulant. Seven patients (33%) showed developmental regression. Most patients had ongoing seizures; however, four of six *SCN1A* variants (67%) in this group (p.V422L, p.I1483M, p.I1498T and p.R1636Q) were associated with a reduction in seizures following SCB treatment (carbamazepine, phenytoin, lamotrigine). There was no reported benefit from SCBs among individuals with the variants p.T226M or p.P1345S. Data for variant carriers p.A420V and p.A1669E revealed mixed responses that were difficult to interpret. No worsening of seizure control was reported with SCB use (Supplementary Table 3 and Supplementary material).

DEE

We report a previously unrecognized *SCN1A* phenotype (p.V1481I; Patient 27). This patient presented after 3 months of age with tonic seizures and subsequent generalized tonic-clonic seizures not triggered by fever and never prolonged. At 7 years of age, the patient had severe intellectual disability; but was ambulant without a MD. He became seizure free with SCBs carbamazepine, oxcarbazepine and lamotrigine (Supplementary Table 3 and Supplementary material) and functional predictions were in keeping with GOF properties (Supplementary Table 1).

GOF NDEEMA versus FHM3 variants cluster in different regions of *SCN1A* channel implicated in inactivation

Following literature review, we identified 11 *SCN1A* variants in families with FHM3 and functionally confirmed GOF properties (phenotypic findings are summarized in Supplementary Table 4). Comparing the 22 early onset DEE and 11 FHM3 variants (Figs 3 and 4), in particular NDEEMA variants were more frequently observed in the S4–5 linker regions (affecting inactivation properties), compared to FHM3 variants that were clustered in the D3–4 linker

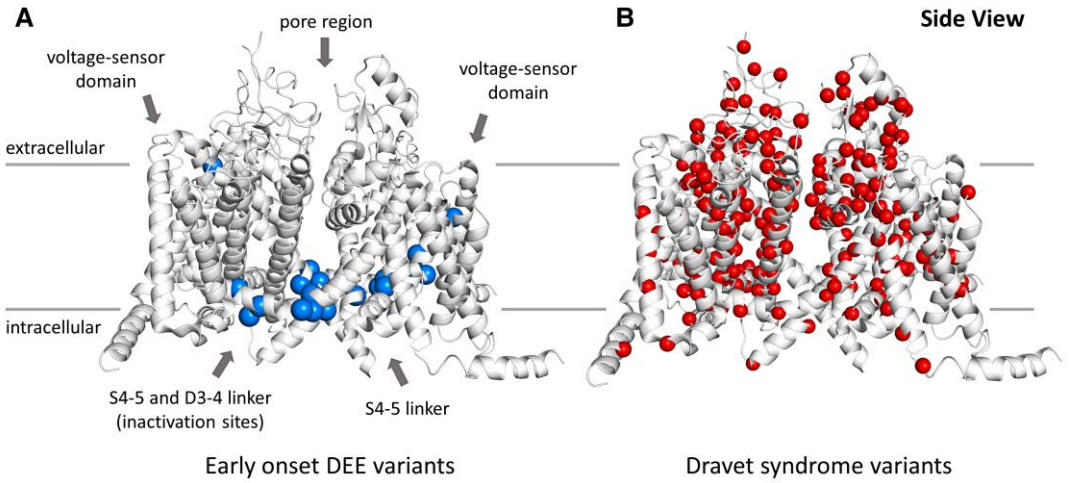

Figure 1 Distribution of early onset DEE versus Dravet syndrome *SCN1A* variants. Transmembrane voltage-gated sodium channel $Na_V1.1$ protein structure in side view with central pore region and pore-loop located at the top (extracellular). Inactivation sites (S4–5 and D3–4 linkers) are located at the bottom (intracellular). (**A**) Early onset DEE missense variants are illustrated in blue. (**B**) Dravet syndrome missense variants are illustrated in red. Early onset DEE variants cluster in regions of channel inactivation (S4–5 and D3–4 linkers) whereas Dravet syndrome variants are frequently located in pore regions (S5–6) (OR = 17.8; CI = 5.4–69.3; $P = 1.3 \times 10^{-7}$).

region (forming the inactivation gate lid; $n = 24$; $z = -3.8$; $r = 0.81$; $P = 8.2 \times 10^{-5}$).

Epilepsy and FHM3 variants display GOF features

We performed functional analyses of the NDEEMA-associated variant p.I236V, the EIDEE/MD-associated variants p.R1636Q and p.I1498T, and the FHM3-associated variant p.I1498M. We transiently transfected human tsA-201 cells with wild-type (WT) human $hNa_V1.1$ or mutant channels, which had been incubated at 37°C for 24 h to record sodium currents by means of whole-cell patch-clamp experiments. Figure 5A–E displays representative current traces of WT and mutant channels elicited with depolarizing voltage steps. The current density of p.I1498M showed a 59% reduction, whereas the other variants did not show statistically significant modifications (although p.R1636Q showed a trend towards reduction, $P = 0.12$). The inactivation curves of p.I1498T and p.I1498M were positively shifted by 6.6 and 16.2 mV, respectively (Fig. 5H and Supplementary Table 5) consistent with a GOF, which is larger for p.I1498M than p.I1498T.

We compared the kinetics of activation and of decay of the current elicited with a depolarizing step to −10 mV (Fig. 6A–D). Exponential fit of the decay shows that the time constant of the mutant p.R1636Q is 7.2-fold slower (Fig. 6E and Supplementary Table 5) consistent with a GOF. The FHM3 mutant p.I1498M was the only one that modified the amplitude of the INa_P, inducing a 2.7-fold increase (Fig. 6F), which is consistent with a GOF. The analysis of the recovery from fast inactivation at −80 mV (Fig. 6G), indicates that the mutants p.R1636Q, p.I1498T and p.I1498M display a faster recovery from fast inactivation, which is consistent with a GOF. The mutants p.R1636Q, p.I1498T and p.I1498M show 36, 37 and 56% decreases in the time constant of recovery, respectively (Fig. 6H).

Because we did not observe statistically significant effects for p.I236V, we evaluated other functional properties for this variant. The current elicited by slow ramp depolarizations (Supplementary Fig. 3A–C) was increased, consistent with GOF. This current can be related both to INap (for which p.I236V showed a mild non-significant trend towards increase) and to features of the kinetics of development of fast inactivation (KDFI). Thus, we evaluated the time constant of the KDFI (Supplementary Fig. 3D–F) and observed a 1.6-fold increase for p.I236V, consistent with increased ramp current and GOF.

FHM3 variants induce larger functional effects than epilepsy variants, in particular causing a substantial increase of persistent Na channel current

We generated radar plots that display the overall differences in functional properties to summarize the functional changes associated with GOF *SCN1A* variants, (Fig. 7). For comparison, we included the p.Q1489K, p.L1649Q and p.L1670W FHM3 variants that we have previously studied.[32–34] Overall, FHM3 variants have larger functional effects than epilepsy variants, in particular, causing a larger increase in INa_P. Interestingly, all the FHM3 variants caused both GOF and LOF effects, in contrast to the epilepsy variants that we have investigated in this study, which selectively induced mild GOF effects.

Action potential-clamp experiments show overall epilepsy and FHM3 variant current increase compared to WT

To reproduce neuronal dynamic conditions during a series of action potentials and to evaluate the overall effect of variants, we performed action potential-clamp experiments recording Na^+ action currents in tsA-201 cells. Notably, these experiments evaluated the overall effect of each variant, with the potential to identify variant-related dysfunction that was not evident in the classical parameters that we had previously characterized.

Our action potential-clamp data showed a large increase in action current amplitude in cells transfected with the FHM3 p.I1498M mutant, and a moderate increase with the mutants involved in epilepsy phenotypes (p.I236V, p.R1636Q and p.I1498T; Fig. 8B–F). In particular, the first action current in the discharge was larger for p.I1498M (2.2-fold increase), whereas the mutants p.I236V, p.R1636Q and p.I1498T did not differ compared to the WT

Figure 2 Features of arthrogryposis in affected individuals. (**A** and **B**) (Patient 4) Contractures in both feet and upper limbs. Right humerus is posteriorly dislocated and left shoulder dysplastic. There are contractures in elbows, wrists and fingers. Ankles are mobile, but a vertical talus can be palpitated. Vertical talus was treated with repeated casting and Achilles tenotomy during infancy. Congenital scoliosis has been treated by prolonged plaster casting/corset and hip subluxation has been corrected surgically. (**C** and **D**) (Patient 3) Bilateral elbow contractures. (**E**) (Patient 1) Hand and finger contractures.

(Fig. 8G). Comparing the mean peak amplitude of the last three action currents in the discharge, we found that all the mutants induced an increase in comparison to the WT, although the action currents of the FHM3 mutant p.I1498M were significantly larger than those of the other mutants (Fig. 8H) (3.8-fold for p.I236V, 2.8-fold for p.R1636Q, 2.5-fold for p.I1498T and 6.3-fold for p.I1498M).

These data show GOF as the overall effect of all the mutants studied, consistent with neuronal hyperexcitability. Notably, the GOF effect was much stronger for the FHM3 mutant p.I1498M in comparison with the epilepsy mutants. Furthermore, the p.Q1489K, p.L1649Q and p.L1670W FHM3 variants that we have previously studied showed a large effect on action currents that was similar to that of p.I1498M.[32–34]

In silico functional predictions of channel function concur with biophysical readouts

Several *in silico* tools were used to aid functional variant estimation of the 33 different early onset DEE and FHM3 *SCN1A* variants presented in this report. Apart from the four variants that were electrophysiologically studied here (p.I236V, p.I1498M, p.I1498T, p.R1636Q), 11 FHM3 variants had previously been functionally identified as GOF (Supplementary Table 1). Seventeen of the remaining 18 variants had either evidence of an identical paralogue in a related sodium channel with GOF properties ($n = 13$) and/or were predicted as GOF by the functional variant prediction tool funNCion ($n = 15$; Supplementary Table 1). Only one patient (Patient 24; p.A420V) had a non-identical *SCN8A* paralogue (p.A408T) with a DEE GOF phenotype, located at a predicted GOF site.[36] Where available, *in silico* functional predictions concurred with biophysical assessments in all cases. On the basis of the paralogue and funNCion assessments and given the homogeneity of the associated phenotypes, these variants were inferred as GOF (Supplementary Table 1).

Discussion

SCN1A related GOF epilepsies—a phenotypic spectrum

While *SCN1A* GOF variants are a well-recognized cause of FHM3, reports have emerged identifying patients with *SCN1A* variants and atypical epilepsy phenotypes.[21,23] A recent study suggests that *SCN1A* GOF variants may account for these findings[22]; however, observations to date have been limited to single patients or small case series, precluding a definitive association between genotype and phenotype.[21,23,38,40] Our comprehensive clinical, genetic and biophysical studies establish that *SCN1A* GOF related disease extends beyond FHM3 phenotypes and encompasses a spectrum of overlapping epilepsy phenotypes. From the most severe neonatal onset DEE with MD and arthrogryposis (NDEEMA), to early infantile (<3 months) DEE with MD and the least severe later onset (≥3 months) DEE without a MD. While there are many similarities in presentation among these three overlapping phenotypes, key distinguishing features are the age at onset, the presence of arthrogryposis and that of a MD. All phenotypes show biophysical evidence of GOF. This finding has significant implications for current and future precision therapies. Diagnosis of novel phenotypes is not only important to aid counselling of currently unexplained cases but guides treatment choice for affected individuals, with most GOF-associated variants responding to sodium channel blocking

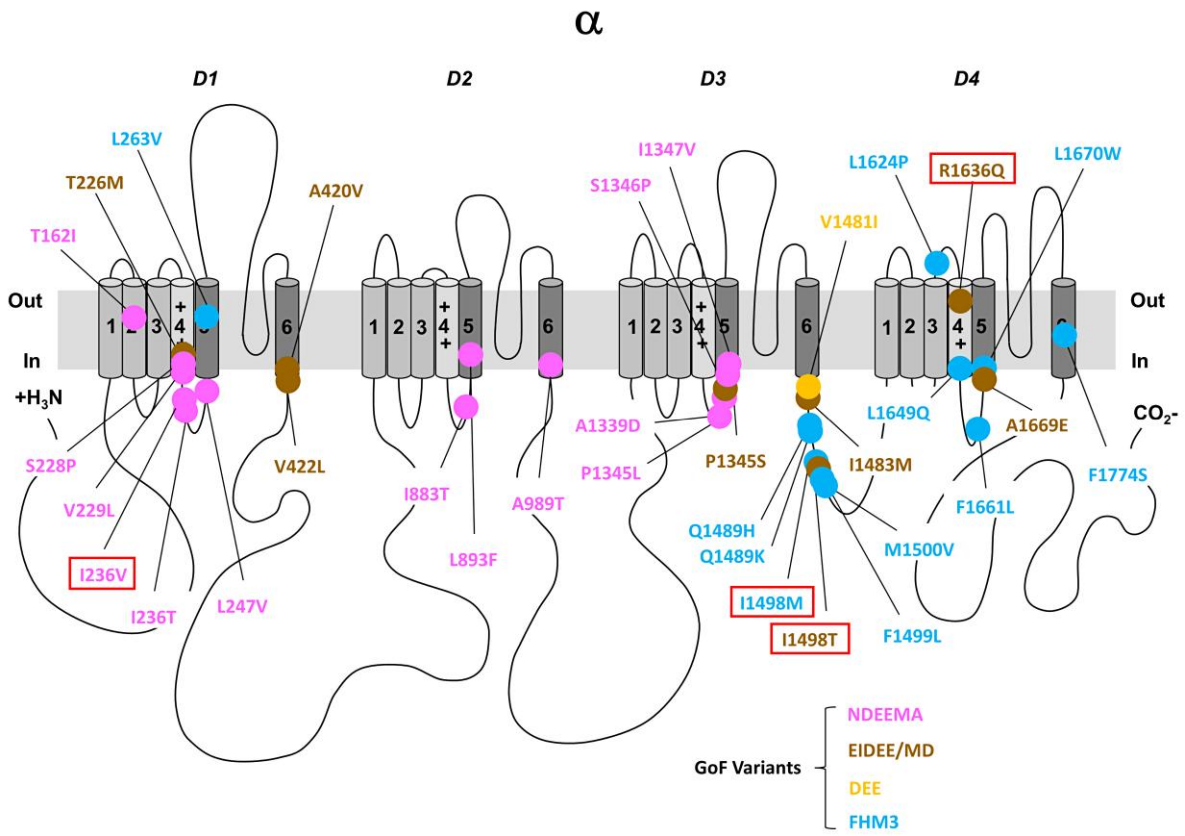

Figure 3 2D representation of GOF variant phenotypes across the SCN1A protein. The alpha subunit consists of four homologous domains (D1–4) each formed of six transmembrane segments (S1–S6). Segment 4 represents the voltage sensor and segments S5–6 the pore region. Individual missense variants are displayed as different coloured circles according to phenotype: Pink denotes NDEEMA, brown denotes EIDEE/MD, amber denotes DEE and blue denotes FHM3. Functionally studied variants are framed in red.

therapies. Therefore, GOF disease should be considered in early onset DEEs with a pathogenic *SCN1A* variant and non-Dravet syndrome phenotype.

Key clinical differences compared to SCN1A LOF epilepsies

The *SCN1A* GOF phenotypes we describe are very different from typical LOF Dravet syndrome and GEFS+ presentations.[12,13,42] Very early neonatal onset seizures in the first days of life accompanied by arthrogryposis are highly specific for the newly described NDEEMA phenotype. Some of these children presented with osteopenia, bone fractures and metabolic acidosis, which is not a feature of Dravet syndrome. Febrile seizures are a hallmark of Dravet syndrome/GEFS+ but are not frequently encountered in GOF-associated phenotypes. Similarly, early EEG features of non-convulsive status epilepticus and continuous spike-wave during sleep are not commonly found in Dravet syndrome. Early evidence of profound intellectual disability paired with the emergence of a prominent MD in the first years of life is highly unusual for Dravet syndrome and more suggestive of a GOF phenotype.[21,22] The mildest form of GOF DEE presented after 3 months of age, however, the presentation was characterized by tonic seizures, not triggered by fever and never prolonged, which makes this presentation clearly distinct from LOF *SCN1A* related Dravet syndrome/GEFS+.

Differing biophysical characteristics of GOF FHM3 versus epilepsy phenotypes

We report the functional characterization of four $hNa_V1.1$/*SCN1A* variants that are responsible for NDEEMA (p.I236V), EIDEE/MD (p.R1636Q and p.I1498T) and FHM3 (p.I1498M). Analysis of the overall effect of the variants on the function of the $hNa_V1.1$ channels by means of action potential-clamp experiments reveals that the alteration of the gating properties induced by the FHM3 p.I1498M variant leads to a large GOF with significant increase of persistent current, similar to the other FHM3 variants we have previously studied (Fig. 7).[32–34] The analysis of the overall effect of the variants p.I236V, p.R1636Q and p.I1498T shows that they induce a more moderate GOF, quantitatively consistent with the only available functional study of a $hNa_V1.1$ EIDEE variant, which induced mixed GOF and LOF effects.[22] Therefore, our data, which directly compare the effect of epilepsy and FHM3 variants, show that variants of $hNa_V1.1$ inducing a mild GOF cause epilepsy, whereas variants inducing a stronger GOF, in particular with a large increase of INa_P, lead to FHM3. Interestingly, our data demonstrate that the change of the amino acid p.I1498 with either a threonine or a methionine induces two different phenotypes (p.I1498T-EIDEE and p.I1498M-FHM3). This indicates that localization of the variant on the primary structure of the channel is not the only parameter that directly correlates with the pathology, and that the physicochemical properties of the amino acid are important in determining the functional effect and phenotype associated with the variant.

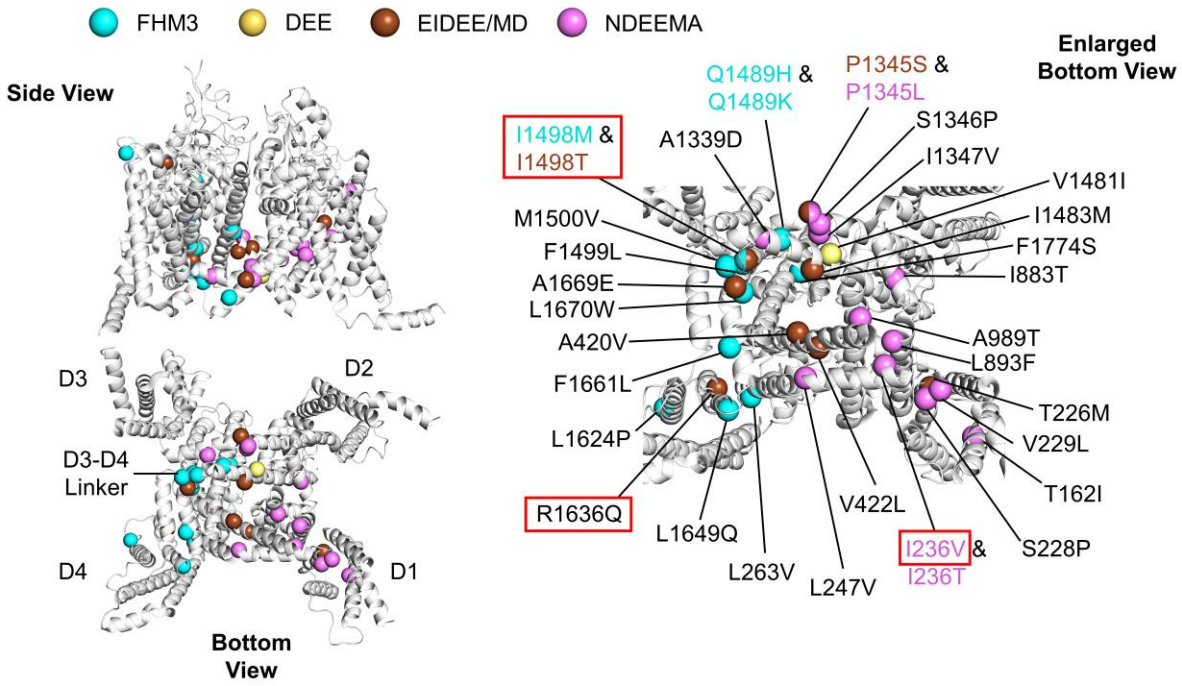

Figure 4 3D representation of GOF *SCN1A* variants. 3D SCN1A protein structure in side (*top left*) and bottom view (*bottom left and right*—enlarged). Individual missense variants are displayed as different coloured circles according to phenotype. Pink denotes NDEEMA, brown denotes EIDEE/MD, amber denotes DEE and blue denotes FHM3. Functionally studied variants are framed in red. NDEEMA variants are more frequently observed in the S4–5 linker regions compared to FHM3 variants that are clustered in the D3–4 linker region ($n = 24$; $z = -3.8$; $r = 0.81$; $P = 8.2 \times 10^{-5}$).

Comparison with Dravet syndrome and GEFS+ $Na_V1.1$ variants

In contrast to NDEEMA and FHM3 variants, Dravet syndrome and GEFS+ $Na_V1.1$-*SCN1A* variants induce LOF.[1,17] About 50–55% of variants associated with Dravet syndrome are truncations/deletions predicted to result in LOF due to non-functional channels. The remainder are missense variants that result in LOF because they reduce the current amplitude generated by the mutant channels and/or modify their gating properties.[43]

Both Dravet syndrome and GEFS+ mouse models reproduce human phenotypes. Through these models, we have understood that $Na_V1.1$ LOF induces hypoexcitability of GABAergic neurons and consequent reduced inhibition in neuronal networks,[9,44] which may be caused by facilitated depolarization block of GABAergic neurons expressing LOF $Na_V1.1$ mutants.[45]

FHM3 variants can induce hyperexcitability of GABAergic neurons, which can facilitate the generation of spreading depolarizations, a pathological mechanism of migraine with aura[46] and a knock-in mouse model of a FHM3 variant shows spreading depolarizations, but not seizures.[47] It is not understood yet how the relatively moderate GOF functional changes in epilepsy $Na_V1.1$ variants can cause such severe phenotypes. We may, however, speculate that the larger GOF of FHM3 variants causes a milder phenotype of hemiplegic migraine instead of epilepsy, because it induces strong hyperexcitability of GABAergic neurons and extracellular K+ accumulation, leading to spreading depolarization of the entire neuronal network as we have shown previously,[45,46] which could block seizure onset. Notably, spreading depolarization has been interpreted as a general anti-seizure mechanism.[48] The milder hyperexcitability induced by the EIDEE variants would not be sufficient to induce spreading depolarization.

Genotype–phenotype associations across the GOF *SCN1A* spectrum

The differences in severity of clinical presentation ranging from NDEEMA to EIDEE and FHM3 appear to be reflected in the respective variant positions across the SCN1A protein. FHM3-associated variants tend to cluster either in the D3–4 linker region forming the hinged lid to occlude the intracellular mouth of the pore or in the S4–5 linker and S6 of domain 4 that form part of the inactivation gate receptor into which the inactivation gate closes to enable channel inactivation.[49] In contrast, NDEEMA variants are frequently observed in intracellular S4–5 linkers, consistent with dysfunction in the coupling between voltage sensing and pore regions of the channel.[49–51] Although the location of variants in particular functional domains appear important, genotype–phenotype associations between these very different disorders appear to be closely related,[1,52] as we observe that a single amino acid change from p.I1498T to p.I1498M is associated with a different disease phenotype: p.I1498T leading to EIDEE/MD and p.I1498M leading to FHM3. We were able to show GOF consistent with neuronal hyperexcitability as the overall effect of all the mutants studied. However, while GOF effects were much stronger for FHM3-associated variants compared with DEE-associated variants, all the FHM3 variants induce both GOF and LOF effects, whereas the epilepsy variants that we have studied selectively induce mild GOF effects. However, mixed GOF and LOF effects were observed for the EIDEE/MD p.T226M variant previously studied.[22] Overall, our findings suggest that the observed biophysical differences between FHM3 and NDEEMA/EIDEE and MD can partially explain the observed clinical differences. However, there may well be other unrecognized factors contributing to this distinction, for example a different genetic background.

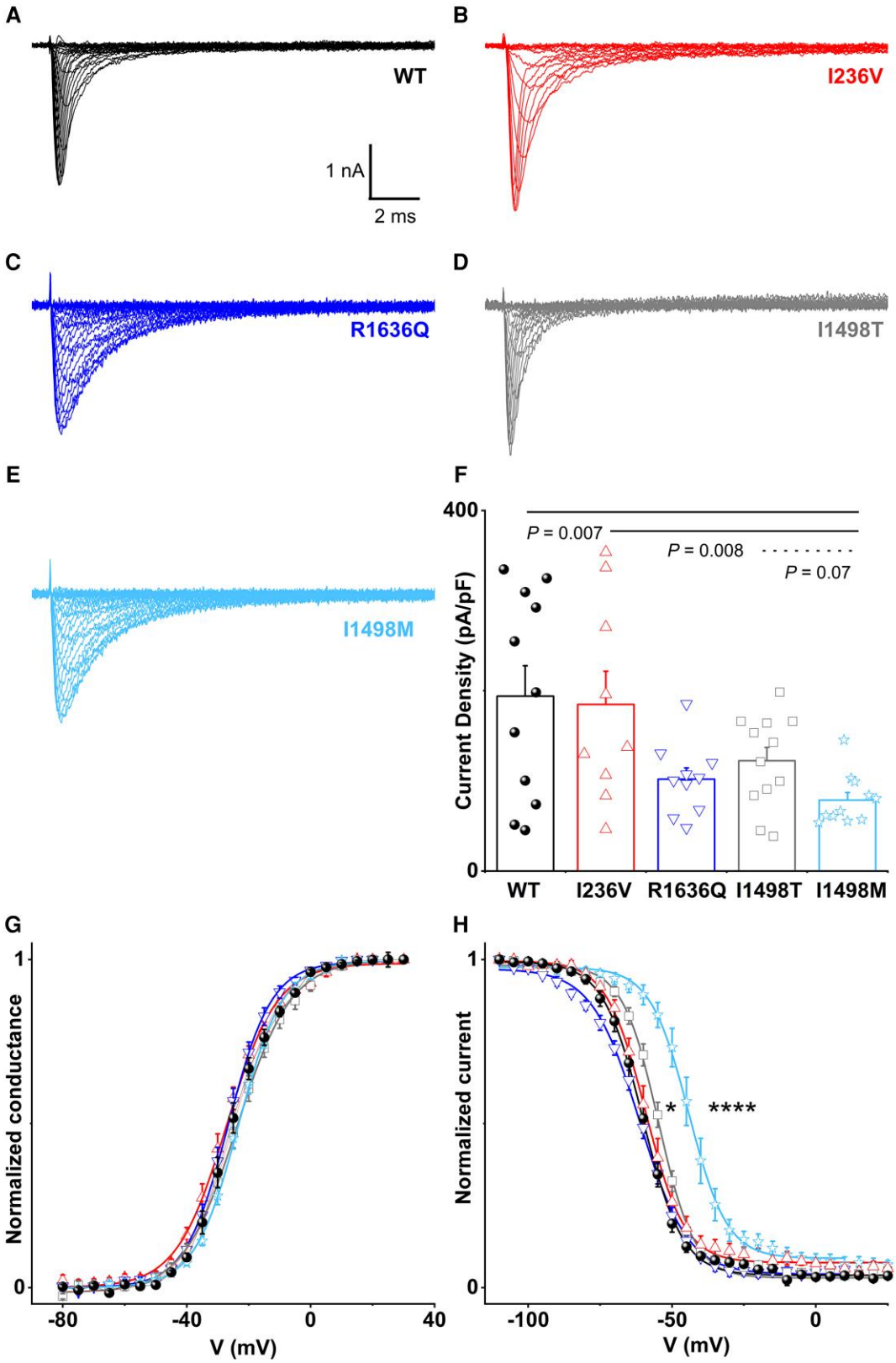

Figure 5 Effects of p.I236V, p.R1636Q, p.I1498M and p.I1498T on voltage-dependent properties of the hNav1.1 channel. Representative whole-cell Na^+ current families for $hNa_v1.1$-WT. (**A**) $hNa_v1.1$-I236V, (**B**) $hNa_v1.1$-R1636Q, (**C**) $hNa_v1.1$-I1498T, (**D** and **E**) $hNa_v1.1$-I1498M, recorded with 100-ms-long depolarizing voltage steps from −80 to +60 mV in 5 mV increments from a holding potential of −100 mV. Scale bars = 1 nA, 2 ms. (**F**) Maximal current density calculated for cells transfected with the WT or the mutants. (**G**) Mean voltage dependence of activation, lines are mean Boltzmann fits. (**H**) Mean voltage dependence of fast inactivation, lines are mean Boltzmann fits. Comparison of mean normalized currents elicited with a 150-ms-long depolarizing step to −10 mV from a holding potential of −100 mV. Data are shown as mean ± SEM. $^*P < 0.05$; $^{****}P < 0.0001$.

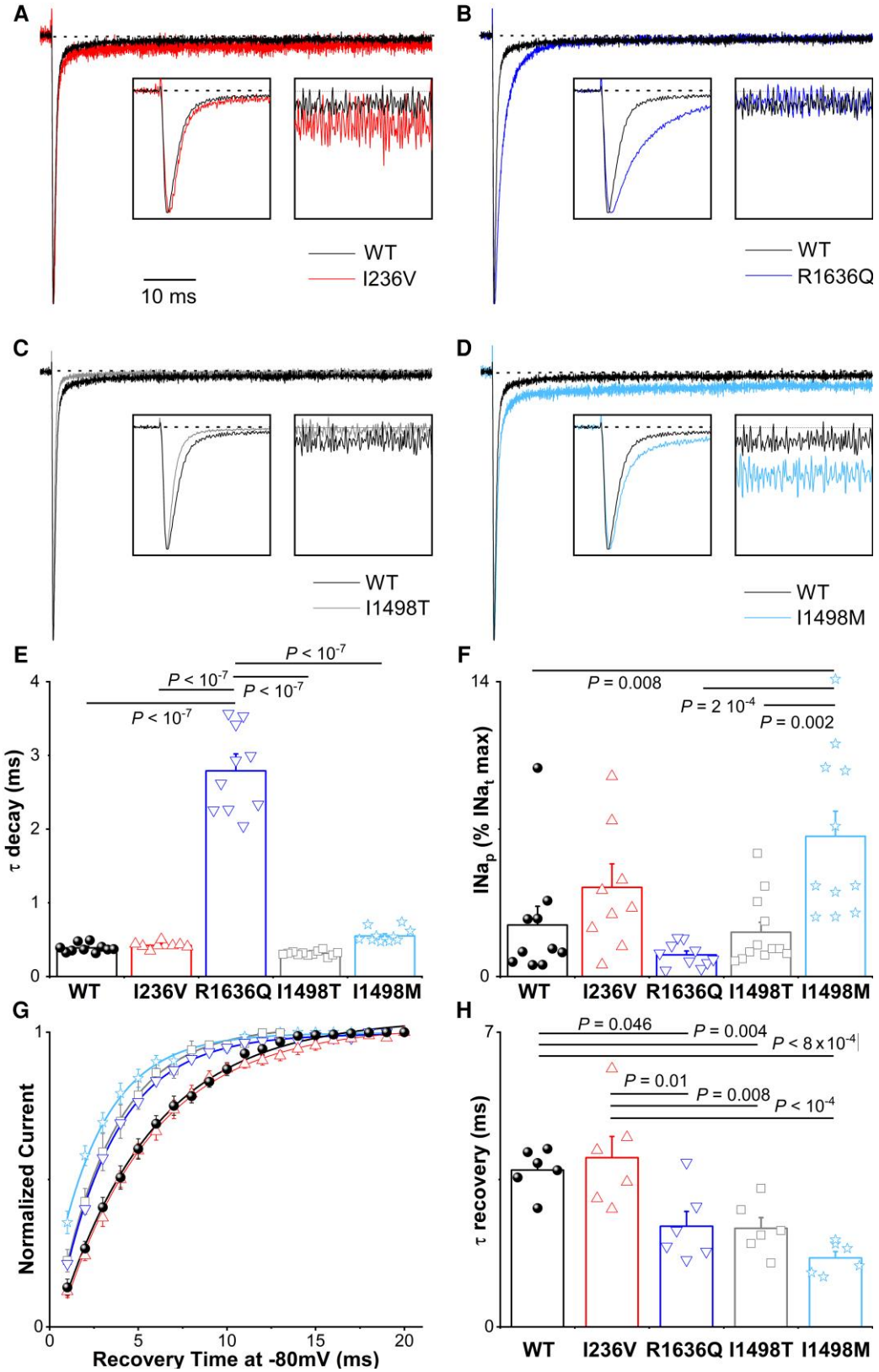

Figure 6 Effects on kinetic properties and persistent current. (**A**) $hNa_v1.1$-WT (black) and $hNa_v1.1$-I236V (red), (**B**) $hNa_v1.1$ (black) and $hNa_v1.1$-R1636Q (blue), (**C**) $hNa_v1.1$ (black) and $hNa_v1.1$-I1498T (light green), (**D**) $hNa_v1.1$-WT (black) and $hNa_v1.1$-I1498M (dark green). Scale bar = 10 ms. The left insets show a 6-ms window of the current traces to compare the current decay and the right insets show the traces between 73.5 and 78.5 ms to compare INap. (**E**) Time constant (τ in ms) of the current decay at −10 mV (single exponential fits at the indicated potentials). (**F**) Quantification of persistent current between 73.5 and 78.5 ms of the 150-ms-long depolarizing step. (**G**) Kinetics of recovery from fast inactivation at −80 mV and (**H**) time constant (τ in ms) of recovery obtained from the exponential fit of the recovery curves. Data are shown as mean ± SEM.

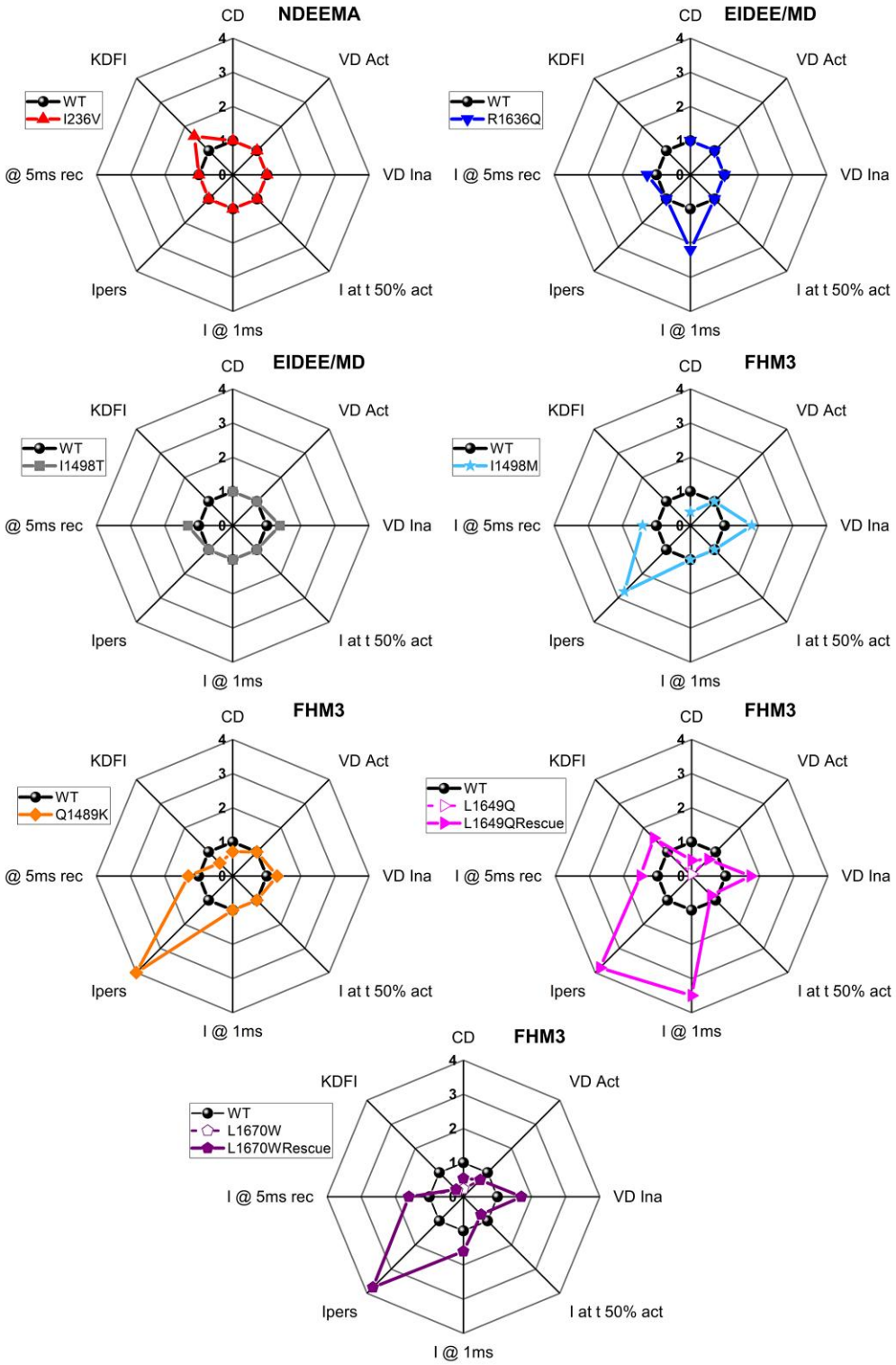

Figure 7 Comparison of the functional effects of epilepsy and FHM3 $Na_V1.1$ variants. The modifications in the studied functional parameters are summarized with radar plots for the variants investigated and for three additional FHM3 variants (Q1489K, L1649Q and L1670W) that we previously investigated.[32–34] To compare meaningful biological modifications, we displayed fold changes in current or conductance in comparison with WT $hNa_V1.1$ for each of the functional parameters that we considered. Thus, values >1 are GOF, values <1 are LOF. CD = maximal current density; VD Act = voltage dependence of activation expressed as fold change in normalized conductance at Va; VD Ina = voltage dependence of inactivation expressed as fold change in normalized conductance at Vh; I at t 50% act (−10 mV) = activation kinetics expressed as fold changes in the current elicited by a −10 mV voltage step at t corresponding to 50% Imax of WT $hNa_V1.1$; I @ 1 ms = kinetics of current decay quantified as fold changes in the current recorded 1 ms after the beginning of a voltage step to −10 mV; Ipers = persistent current; I @ 5 ms rec = kinetics of recovery from fast inactivation expressed as fold changes in current after 5 ms of recovery at −80 mV. KDFI = kinetics of development of fast inactivation. Holding potential was −100 mV for all the conditions. Slope factors of activation and inactivation were not included because their modifications do not directly induce net gain or LOF effects.

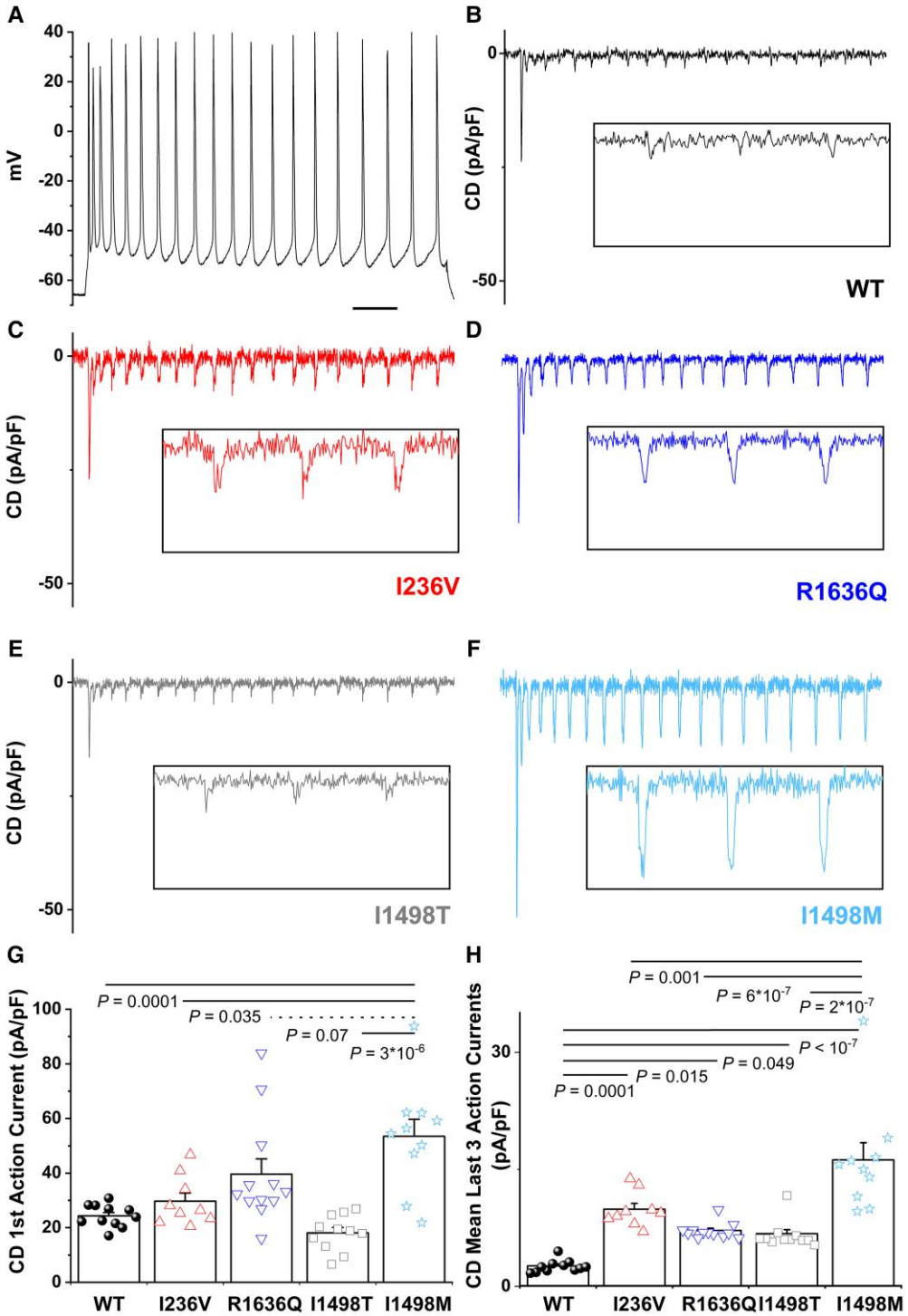

Figure 8 Overall effect of the variants evaluated with action potential-clamp experiments. Action Na^+ currents (expressed as mean of conductance, error bars are not shown for clarity) recorded using as voltage stimulus an action potential discharge (**A**) recorded in a neuron in neocortical slices for (**B**) $hNa_v1.1$-WT, (**C**) $hNa_v1.1$-I236V, (**D**) $hNa_v1.1$-R1636Q, (**E**) $hNa_v1.1$-I1498T and (**F**) $hNa_v1.1$-I1498M. Scale bar = 20 ms. (**G**) Comparison of the current density of the first action current. (**H**) Comparison of the current density of the mean of the three last action currents. Data are shown as mean ± SEM.

Disease paralogues and functional *in silico* tools contribute to $Na_V1.1$ effect prediction

Variants that are equivalent to the ones investigated in this study have been identified in paralogue sodium channels. Here we reported a variant affecting the outermost arginine in the IVS4 voltage sensor in $Na_V1.1$ (p.R1636Q, this study). A paralogous variant in the cardiac isoform $Na_V1.5$-SCN5A (p.R1623Q) is associated with long QT syndrome,[53] and in a paralogous variant in $Na_V1.6$ (p.R1617Q) is associated with early infantile epileptic encephalopathy.[54] A slower current decay was observed in all three variants inducing a GOF by destabilizing the inactivated state, consistent with

the role of this arginine residue in the generation of conformational changes that initiate sodium channel inactivation,[55] although detailed effects on gating properties are isoform specific. Comparison of variants in paralogue genes can facilitate prediction of functional effects for sodium channel variants (Supplementary Table 1), although specific gating dysfunctions may vary. This observation is supported by recent work showing that variant paralogues across *SCN*s display similar functional effects implying that variant functional effect and location within one voltage-gated sodium channel can serve as a surrogate for variant effects across related sodium channels.[7,35] We observed consistent agreement between biophysical readouts, *SCN* paralogue details and functional estimation via the *in silico* prediction tool funNCion, on the basis of a large dataset of voltage-gated sodium and calcium channel presentations.[36] Given the limited predictive certainty of the *funNCion* tool, paralogue variants should be weighted higher for the functional prediction.

Most GOF *SCN1A* variant carriers respond to sodium channel blocking therapies

Nearly all patients in this GOF *SCN1A* cohort had epilepsy that was very difficult to treat and were exposed to multiple anti-seizure medications. A major finding of our study is that the majority of patients who received SCB treatment reported seizure reduction and none reported exacerbation of seizures. This was particularly the case for the NDEEMA phenotypes, nearly all of whom responded to SCB. Our results are consistent with the beneficial use of SCBs in other GOF sodium channel epilepsies including *SCN2A*, *SCN3A* and *SCN8A* associated disorders.[3,4,6,56]

Not all patients in our cohort responded to SCB use and higher doses of SCBs might be required in some individuals as previously shown for GOF *SCN2A* and *SCN8A* related epilepsies.[3,57] A number of individuals with EIDEE/MD phenotypes nevertheless appeared refractory to SCBs use. For example, none of the 10 patients with the p.T226M variant reported a response to SCBs. This may relate to the complex underlying biophysical properties of the p.T226M variant.[21,22] This variant has GOF effects, including a hyperpolarizing shift in activation; however, this is accompanied by a hyperpolarizing shift in inactivation. The net consequence in rapid firing cells was entry into depolarizing block, where cells were no longer able to fire action potentials resulting in mixed GOF and LOF. Ultimately, treatment responsiveness appears to be closely related to the underlying biophysical properties of the specific variant.

Recent advances in disease modifying treatments for Dravet syndrome target specifically the underlying LOF disease mechanism, aiming to restore the expression of Nav1.1 channels.[24] While this novel approach may be beneficial for LOF disease, mechanisms that upregulate *SCN1A* expression could exacerbate and worsen GOF disorders. Potential disease modifying approaches to GOF disorders would aim to downregulate *SCN1A* expression.

In view of these novel therapeutic developments, it is particularly important to ensure that GOF *SCN1A* spectrum disorders are diagnosed early. This will enable appropriate counselling regarding the severity of the disease spectrum and guide treatment options with SCBs.

There are several limitations to this study. Due to the novelty of the presented disease phenotypes, we were not able to collect data prospectively but relied on retrospective data collection by clinicians using original medical records. Given that functional experiments on *SCN1A* mutants are complex and labour intensive we were unable to biophysically characterize all disease variants presented in this study. Instead, we focused our analysis on representative variants associated with the here presented disease spectrum, including recurring variants (p.R1636Q) and variants affecting the same amino acid residue associated with differing phenotypes (p.I1498M, p.I1498T). We show that *in silico* functional predictions concurred with biophysical assessments (Supplementary Table 1), illustrating that disease paralogues and *in silico* functional tools can be valid surrogate measures for channel function.

Conclusion

This study establishes that *SCN1A* GOF variants are associated with a disease spectrum ranging from the previously undescribed severe NDEEMA, to EIDEE/MD and the milder FHM3. Recognition of key presenting features will prevent misdiagnosis and guide treatment choice towards sodium channel blocking therapies.

Acknowledgements

We would like to thank the Dravet Syndrome Foundation (grant number 272016) and Dravet Syndrome UK (grant number 16GLW00) for their generous grants to support this work.

Funding

D.L.'s work was supported by funds from the Dravet Syndrome Foundation (grant number, 272016), the BMBF (Treat-ION grant, 01GM1907), NIH NINDS (Channelopathy-Associated Epilepsy Research Center, 5-U54-NS108874). A.B. and S.M.Z. received a grant from Dravet Syndrome UK for the Glasgow *SCN1A* database (grant number 16GLW00). M.M. and S.C.'s work was supported by the Laboratory of Excellence 'Ion Channel Science and Therapeutics' (LabEx ICST, ANR-11-LABX-0015-01, France), by the Foundation Famiglie Dravet ONLUS—Italy (FDO-2018) and by IDEX UCA-Jedi (University Côte d'Azur ANR-15-IDEX-01, France). This work is supported by the NIHR GOSH BRC. The views expressed are those of the author(s) and not necessarily those of the NHS, the NIHR or the Department of Health. The funders had no role in the design and conduct of the study; collection, management, analysis, and interpretation of the data; preparation, review, or approval of the manuscript; and decision to submit the manuscript for publication.

Competing interests

A.A. has served as principal investigator or member of DMCs in clinical trials for Eisai, UCB, GW Pharma; received consulting fees from GW Pharma, Zogenix, Eisai, Takeda, Biocodex, Encoded Therapeutics; unrestricted research grants from UCB, Caixa Foundation and GW Pharma and academic research grants from EJP-RD and the EU. A.B. has received honoraria for presenting at educational events, advisory boards and consultancy work for Biocodex, GW Pharma, Encoded Therapeutics, Stoke Therapeutics, Nutricia and Zogenix. D.L. has received honoraria for advisory board work for Encoded Therapeutics. M.M. has received honoraria for presenting at educational events from Zogenix and UCB. E.P.P. has received honoraria for consultancy work for the Friends of Faces foundation. S.P. has received honoraria for consulting from Greenwich Biosciences, Zogenix, Stoke Therapeutics, Encoded Therapeutics, Neurelis, Taysha and Marinus. He has received honoraria for speaker bureaus for

Greenwich Biosciences, and Zogenix. K.P. has served on advisory board for Roche. I.E.S. has served on scientific advisory boards for UCB, Eisai, GlaxoSmithKline, BioMarin, Nutricia, Rogcon, Chiesi, Encoded Therapeutics, Knopp Biosciences and Xenon Pharmaceuticals; has received speaker honoraria from GlaxoSmithKline, UCB, BioMarin, Biocodex, Chiesi, Liva Nova and Eisai; has received funding for travel from UCB, Biocodex, GlaxoSmithKline, BioMarin and Eisai; has served as an investigator for Zogenix, Zynerba, Ultragenyx, GW Pharma, UCB, Eisai, Xenon Pharmaceuticals, Anavex Life Sciences, Ovid Therapeutics, Epigenyx, Encoded Therapeutics and Marinus; and has consulted for Zynerba Pharmaceuticals, Atheneum Partners, Ovid Therapeutics, Care Beyond Diagnosis, Epilepsy Consortium and UCB. She may accrue future revenue on pending patent WO61/010176 (filed: 2008): Therapeutic Compound; has a patent for SCN1A testing held by Bionomics Inc and licensed to various diagnostic companies; has a patent molecular diagnostic/theranostic target for benign familial infantile epilepsy (BFIE) [PRRT2] 2011904493 and 2012900190 and PCT/AU2012/001321 (TECH ID:2012-009). S.S. receives funding by the Dietmar Hopp Stiftung (1DH1813319). E.W. is DSMB for Encoded, Acadia, Amicus and Neurocrine and has received consulting fees from BioMarin. S.M.Z. has received honoraria for presenting at educational events, advisory boards and consultancy work for GW Pharma, Zogenix, Biocodex, Encoded Therapeutics, Stoke Therapeutics and Nutricia. No other disclosures were reported.

Supplementary material

Supplementary material is available at *Brain* online.

References

1. Mantegazza M, Cestèle S, Catterall WA. Sodium channelopathies of skeletal muscle and brain. *Physiol Rev*. 2021;101:1633–1689.
2. Claes L, Del-Favero J, Ceulemans B, Lagae L, Van Broeckhoven C, De Jonghe P. De novo mutations in the sodium-channel gene SCN1A cause severe myoclonic epilepsy of infancy. *Am J Hum Genet*. 2001;68:1327–1332.
3. Wolff M, Johannesen KM, Hedrich UBS, *et al*. Genetic and phenotypic heterogeneity suggest therapeutic implications in SCN2A-related disorders. *Brain*. 2017;140:1316–1336.
4. Larsen J, Carvill GL, Gardella E, *et al*. The phenotypic spectrum of SCN8A encephalopathy. *Neurology*. 2015;84:480–489.
5. Veeramah KR, O'Brien JE, Meisler MH, *et al*. De novo pathogenic SCN8A mutation identified by whole-genome sequencing of a family quartet affected by infantile epileptic encephalopathy and SUDEP. *Am J Hum Genet*. 2012;90:502–510.
6. Zaman T, Helbig I, Božović IB, *et al*. Mutations in SCN3A cause early infantile epileptic encephalopathy. *Ann Neurol*. 2018;83:703–717.
7. Brunklaus A, Du J, Steckler F, *et al*. Biological concepts in human sodium channel epilepsies and their relevance in clinical practice. *Epilepsia*. 2020;61:387–399.
8. Escayg A, MacDonald BT, Meisler MH, *et al*. Mutations of SCN1A, encoding a neuronal sodium channel, in two families with GEFS +2. *Nat Genet*. 2000;24:343–345.
9. Yu FH, Mantegazza M, Westenbroek RE, *et al*. Reduced sodium current in GABAergic interneurons in a mouse model of severe myoclonic epilepsy in infancy. *Nat Neurosci*. 2006;9:1142–1149.
10. Ogiwara I, Miyamoto H, Morita N, *et al*. Nav1.1 localizes to axons of parvalbumin-positive inhibitory interneurons: A circuit basis for epileptic seizures in mice carrying an Scn1a gene mutation. *J Neurosci*. 2007;27:5903–5914.
11. Dravet C, Bureau M, Oguni H, Fukuyama Y, Cokar O. Severe myoclonic epilepsy in infancy: Dravet syndrome. *Adv Neurol*. 2005;95:71–102.
12. Brunklaus A, Ellis R, Reavey E, Forbes GH, Zuberi SM. Prognostic, clinical and demographic features in SCN1A mutation-positive Dravet syndrome. *Brain*. 2012;135:2329–2336.
13. Zhang YH, Burgess R, Malone JP, *et al*. Genetic epilepsy with febrile seizures plus: Refining the spectrum. *Neurology*. 2017;89:1210–1219.
14. Brunklaus A, Zuberi SM. Dravet syndrome—From epileptic encephalopathy to channelopathy. *Epilepsia*. 2014;55:979–984.
15. Brunklaus A, Schorge S, Smith AD, *et al*. SCN1A variants from bench to bedside-improved clinical prediction from functional characterization. *Hum Mutat*. 2020;41:363–374.
16. Guerrini R, Dravet C, Genton P, Belmonte A, Kaminska A, Dulac O. Lamotrigine and seizure aggravation in severe myoclonic epilepsy. *Epilepsia*. 1998;39:508–512.
17. Mantegazza M, Broccoli V. SCN1A/NaV1.1 channelopathies: Mechanisms in expression systems, animal models, and human iPSC models. *Epilepsia*. 2019;60(S3):S25–S38.
18. Dichgans M, Freilinger T, Eckstein G, *et al*. Mutation in the neuronal voltage-gated sodium channel SCN1A in familial hemiplegic migraine. *Lancet*. 2005;366:371–377.
19. Vahedi K, Depienne C, Le Fort D, *et al*. Elicited repetitive daily blindness: a new phenotype associated with hemiplegic migraine and SCN1A mutations. *Neurology*. 2009;72:1178–1183.
20. Mantegazza M, Cestèle S. Pathophysiological mechanisms of migraine and epilepsy: similarities and differences. *Neurosci Lett*. 2018;667:92–102.
21. Sadleir LG, Mountier EI, Gill D, *et al*. Not all SCN1A epileptic encephalopathies are Dravet syndrome: Early profound Thr226Met phenotype. *Neurology*. 2017;89:1035–1042.
22. Berecki G, Bryson A, Terhag J, *et al*. SCN1A gain of function in early infantile encephalopathy. *Ann Neurol*. 2019;85:514–525.
23. Jaber D, Gitiaux C, Blesson S, *et al*. *De novo* mutations of SCN1A are responsible for arthrogryposis broadening the SCN1A-related phenotypes. *J Med Genet*. 2021;58:737–742.
24. Han Z, Chen C, Christiansen A, *et al*. Antisense oligonucleotides increase Scn1a expression and reduce seizures and SUDEP incidence in a mouse model of Dravet syndrome. *Sci Transl Med*. 2020;12:eaaz6100.
25. Scheffer IE, Berkovic S, Capovilla G, *et al*. ILAE classification of the epilepsies: Position paper of the ILAE Commission for Classification and Terminology. *Epilepsia*. 2017;58:512–521.
26. Fisher RS, Cross JH, French JA, *et al*. Operational classification of seizure types by the International League Against Epilepsy: Position Paper of the ILAE Commission for Classification and Terminology. *Epilepsia*. 2017;58:522–530.
27. Richards S, Aziz N, Bale S, *et al*. Standards and guidelines for the interpretation of sequence variants: A joint consensus recommendation of the American College of Medical Genetics and Genomics and the Association for Molecular Pathology. *Genet Med*. 2015;17:405–424.
28. Rentzsch P, Witten D, Cooper GM, Shendure J, Kircher M. CADD: Predicting the deleteriousness of variants throughout the human genome. *Nucleic Acids Res*. 2019;47(D1):D886–D894.
29. Ioannidis NM, Rothstein JH, Pejaver V, *et al*. REVEL: An ensemble method for predicting the pathogenicity of rare missense variants. *Am J Hum Genet*. 2016;99:877–885.

30. Brunklaus A, Pérez-Palma E, Ghanty I, *et al*. Development and validation of a prediction model for early diagnosis of SCN1A-related epilepsies. *Neurology*. 2022;98:e1163–e1174.
31. Mantegazza M, Gambardella A, Rusconi R, *et al*. Identification of an Nav1.1 sodium channel (SCN1A) loss-of-function mutation associated with familial simple febrile seizures. *Proc Natl Acad Sci USA*. 2005;102:18177–18182.
32. Cestèle S, Scalmani P, Rusconi R, Terragni B, Franceschetti S, Mantegazza M. Self-limited hyperexcitability: Functional effect of a familial hemiplegic migraine mutation of the Nav1.1 (SCN1A) Na^+ channel. *J Neurosci*. 2008;28:7273–7283.
33. Cestèle S, Schiavon E, Rusconi R, Franceschetti S, Mantegazza M. Nonfunctional NaV1.1 familial hemiplegic migraine mutant transformed into gain of function by partial rescue of folding defects. *Proc Natl Acad Sci USA*. 2013;110:17546–17551.
34. Dhifallah S, Lancaster E, Merrill S, Leroudier N, Mantegazza M, Cestele S. Gain of function for the SCN1A/hNav1.1-L1670W mutation responsible for familial hemiplegic migraine. *Front Mol Neurosci*. 2018;11:232.
35. Brunklaus A, Feng T, Brünger T, *et al*. Gene variant effects across sodium channelopathies predict function and guide precision therapy. *Brain*. Published online 17 January 2022. doi:10.1093/brain/awac006.
36. Heyne HO, Baez-Nieto D, Iqbal S, *et al*. Predicting functional effects of missense variants in voltage-gated sodium and calcium channels. *Sci Transl Med*. 2020;12:eaay6848.
37. Pérez-Palma E, May P, Iqbal S, *et al*. Identification of pathogenic variant enriched regions across genes and gene families. *Genome Res*. 2020;30:62–71.
38. Spagnoli C, Frattini D, Rizzi S, Salerno GG, Fusco C. Early infantile SCN1A epileptic encephalopathy: Expanding the genotype-phenotype correlations. *Seizure*. 2019;65:62–64.
39. Ohashi T, Akasaka N, Kobayashi Y, *et al*. Infantile epileptic encephalopathy with a hyperkinetic movement disorder and hand stereotypies associated with a novel SCN1A mutation. *Epileptic Disord*. 2014;16:208–212.
40. Trump N, McTague A, Brittain H, *et al*. Improving diagnosis and broadening the phenotypes in early-onset seizure and severe developmental delay disorders through gene panel analysis. *J Med Genet*. 2016;53:310–317.
41. Freilich ER, Jones JM, Gaillard WD, *et al*. Novel SCN1A mutation in a proband with malignant migrating partial seizures of infancy. *Arch Neurol*. 2011;68:665–671.
42. Dravet C, Oguni H. Dravet syndrome (severe myoclonic epilepsy in infancy). *Handb Clin Neurol*. 2013;111:627–633.
43. Zuberi SM, Brunklaus A, Birch R, Reavey E, Duncan J, Forbes GH. Genotype-phenotype associations in SCN1A-related epilepsies. *Neurology*. 2011;76:594–600.
44. Hedrich UB, Liautard C, Kirschenbaum D, *et al*. Impaired action potential initiation in GABAergic interneurons causes hyperexcitable networks in an epileptic mouse model carrying a human Na(V)1.1 mutation. *J Neurosci*. 2014;34:14874–14889.
45. Lemaire L, Desroches M, Krupa M, Pizzamiglio L, Scalmani P, Mantegazza M. Modeling NaV1.1/SCN1A sodium channel mutations in a microcircuit with realistic ion concentration dynamics suggests differential GABAergic mechanisms leading to hyperexcitability in epilepsy and hemiplegic migraine. *PLoS Comput Biol*. 2021;17:e1009239.
46. Chever O, Zerimech S, Scalmani P, *et al*. Initiation of migraine-related cortical spreading depolarization by hyperactivity of GABAergic neurons and NaV1.1 channels. *J Clin Invest*. 2021;131:e142203.
47. Jansen NA, Dehghani A, Linssen MML, Breukel C, Tolner EA, van den Maagdenberg AMJM. First FHM3 mouse model shows spontaneous cortical spreading depolarizations. *Ann Clin Transl Neurol*. 2020;7:132–138.
48. Tamim I, Chung DY, de Morais AL, *et al*. Spreading depression as an innate antiseizure mechanism. *Nat Commun*. 2021;12:2206.
49. Catterall WA. From ionic currents to molecular mechanisms: The structure and function of voltage-gated sodium channels. *Neuron*. 2000;26:13–25.
50. Payandeh J, Scheuer T, Zheng N, Catterall WA. The crystal structure of a voltage-gated sodium channel. *Nature*. 2011;475:353–358.
51. Catterall WA. Structure and function of voltage-gated sodium channels at atomic resolution. *Exp Physiol*. 2014;99:35–51.
52. Brunklaus A, Ellis R, Reavey E, Semsarian C, Zuberi SM. Genotype phenotype associations across the voltage-gated sodium channel family. *J Med Genet*. 2014;51:650–658.
53. Kambouris NG, Nuss HB, Johns DC, Marbán E, Tomaselli GF, Balser JR. A revised view of cardiac sodium channel 'blockade' in the long-QT syndrome. *J Clin Invest*. 2000;105:1133–1140.
54. Wagnon JL, Barker BS, Hounshell JA, *et al*. Pathogenic mechanism of recurrent mutations of SCN8A in epileptic encephalopathy. *Ann Clin Transl Neurol*. 2016;3:114–123.
55. Chanda B, Bezanilla F. Tracking voltage-dependent conformational changes in skeletal muscle sodium channel during activation. *J Gen Physiol*. 2002;120:629–645.
56. Johannesen KM, Liu Y, Koko M, *et al*. Genotype-phenotype correlations in SCN8A-related disorders reveal prognostic and therapeutic implications. *Brain*. 2022;145(9):2991–3009.
57. Boerma RS, Braun KP, van den Broek MP, *et al*. Remarkable phenytoin sensitivity in 4 children with SCN8A-related epilepsy: A molecular neuropharmacological approach. *Neurotherapeutics*. 2016;13:192–197.